J Mater Sci (2008) 43:6453–6458
DOI 10.1007/s10853-008-2981-7

Self-assembly of polystyrene microspheres within spatially confined rectangular microgrooves

Shih-Kai Wu · Tzu-Piao Tang · Wenjea J. Tseng

Received: 14 May 2008 / Accepted: 2 September 2008 / Published online: 20 September 2008

Abstract A convective self-assembly of mono-sized polystyrene spheres with diameters ranging from 262 to 1000 nm was conducted on patterned silicon wafers with one-dimensional, periodic rectangular microgrooves of different widths (0.65–6 μm). The latex beads were driven into the spatially confined microgrooves by the capillary interactions and the confined wall during solvent evaporation, resulting in a range of packing structures. Processing variables including evaporation temperature, particle size (D), groove width (W), and groove height (H) were examined experimentally, and geometrical models were proposed to explain the various packing structures obtained. The degree of spatial freedom for the particles to rearrange themselves in the confined channels is found critical to the assembled particle-packing structure.

Introduction

Monodisperse polystyrene beads and silica colloids are often used as building blocks for fabricating synthetic opals with long-range periodicity via bottom-up, self-assembly route [1–9], creating ordered structures with a precision that challenges current lithographic techniques for three-dimensional photonic applications [10–12]. In order to grow artificial opals from the colloidal dispersion, an external force field such as gravitational settling [1], electrophoresis [2], and convective evaporation [3] is often used to facilitate a collective deposition of colloidal particles on flat substrate with desired packing configurations. The convective method in particular is characterized by the evaporation of solvent, by which a solvent influx takes place from the solvent-rich (thick) region to the solid–liquid interface (thin region) on the substrate [3, 4]. The convective motion brings colloidal spheres toward the liquid–substrate interface. In the mean time, the top surface of colloidal spheres in an area becomes protruding from the liquid layer as solvent liquid evaporates, the capillary attraction due to menisci formed around the colloidal particles leads to the formation of a nucleus [4]. The menisci formed around the protruding spheres in the nucleus give rise to local capillary forces that in turn also bring in a solvent influx from the thicker areas encircling the nucleus toward the nucleus region. This influx motion advances the interface by reclaiming the loss of liquid solvent, resulting in an iridescent array of orderly packed particle arrangement.

Structures other than the close-packing configuration are yet difficult to achieve via the colloidal self-assembly route, and are hence a subject of some recent research papers [5–7, 9]. Fabrication of colloidal crystals with a tailored particle-packing geometry and most desirably a controlled defect type, defect concentration, and location has been attempted via the use of patterned substrates as a template to guide the opal formation. For example, Xia and co-workers [5] etched rectangular grooves on glass substrate so that polymer beads were allowed to settle into grooves by capillary force. This deposition operation was then followed by heating the polymer beads slightly above their glass transition temperature. A subsequent removal of

S.-K. Wu · W. J. Tseng (✉)
Department of Materials Science and Engineering, National Chung Hsing University, 250 Kuo Kuang Rd., Taichung 402, Taiwan
e-mail: wenjea@dragon.nchu.edu.tw

T.-P. Tang
Department of Materials and Mineral Resources Engineering, National Taipei University of Technology, Taipei 104, Taiwan

the substrate template resulted in free-standing zigzag chains of polymer beads. Hoogenboom et al. [6] designed pillar-shaped templates with a periodical arrangement having the same hole size as that of silica spheres to be arrayed. Large areas of defect-free, symmetric monolayers of ordered vacancy arrays, and body-centered cubic and simple cubic colloidal crystals were grown successfully on the templates. Ozin et al. [7, 8] used V-shaped grooves as a template to grow silica colloidal crystals. The particle-packing configuration was a face-centered cubic (fcc) (100) structure. As the grooves changed to a rectangular shape, the packing configuration transformed into an fcc (111) structure. This reveals that a change of groove shape was able to shed lights in tailoring the crystalline packing structure via the template-assisted colloidal assembly route.

Even though the particle-packing structure of colloidal assemblage appears to depend critically on the template geometry used in the template-assisted self-assembly [5–8], related reference regarding opal formation with geometrical confinement is not extensive. Ye et al. [9] have used substrate with a periodic one-dimensional grating structure as a template for the growth of two-dimensional synthetic opals, and reported that the particle-packing structures strongly depend on the ratio between the diameter of colloidal spheres and the period of the grating. Nonetheless, detailed assembly structures when the ratio of sphere diameter and groove width (and height) varies are yet not well understood. In this regard, silicon wafers with one-dimensional rectangular channels are used as a template in the study for the convective deposition of monodispersed polymer beads via the colloidal self-assembly route. The rectangular grooves were designed such that the long axis of the grooves is placed parallel to the drying direction during solvent evaporation, and the length of the groove is substantially greater than the diameter of polymer beads so that the boundary effect (along the longitudinal direction) to the packing structure of polymer beads can be ignored. Effect of the confined walls to the convective self-assembly is hence restricted to the direction perpendicular to the drying direction only. Process variables such as deposition temperature, sphere size, and width of the rectangular grooves were varied in order to examine their inter-relations with the grown array structure.

Experimental procedure

Mono-sized polystyrene latex beads dispersed in aqueous solution (including spheres of 262, 300, 482, and 1000 nm in diameter, respectively) were used in the study (Ted Pella, Inc., USA). The original solids fraction of 0.1 vol.% were diluted to 0.01 vol.% by addition of deionized water (14 MΩ). The diluted latex solutions were homogenized ultrasonically (Sonicator 3000, Misonix, USA), and filled into a square transparent box with silicon wafers positioned vertically inside the box (Fig. 1). Rectangular microgrooves of different widths (650, 4000, and 6000 nm, respectively) were prepared by photolithography and etching of the silica layer on silicon wafers. Depth of the grooves (H) was held constant at 550 nm. The patterned silica-silicon wafers were repeatedly washed in deionized water and then in acetone for three times prior the deposition process. The transparent box containing the colloidal solutions and the sectioned wafer substrates (all with an equal size of 10 × 15 mm) was placed into a controlled temperature and humidity chamber (KCL-2000A, Tokyo Rikakikai Co., Japan). Three evaporation temperatures were used in the experiment: 30, 45, and 65 °C. A thermocouple was placed near the wafers to verify the evaporation temperature during the assembly process.

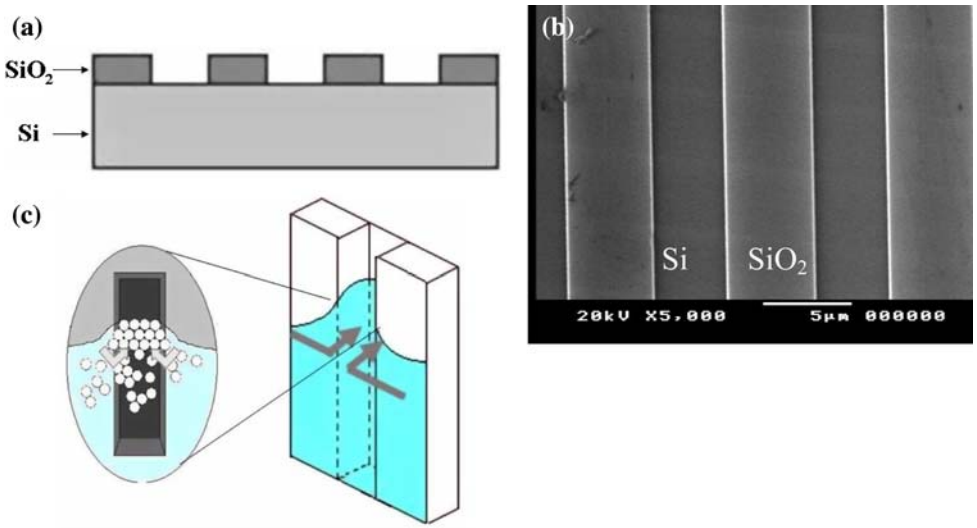

Fig. 1 Schematic of the patterned silicon wafers used to proceed vertical deposition of colloidal latex spheres via convective evaporation. The etched microgrooves are of silica layers (**a**) with rectangular gratings (**b**). (**c**) The latex spheres were driven into the grooves by capillary forces at the liquid–solid interface

Relative humidity was held at 60% throughout the experiment. Measurement of dihedral angle (FTA2000, First Ten Ångstroms, USA) on bare silicon wafer and un-etched silica-top wafers showed that the contact angle was 46.6° for water-silicon interface and 59.7° for water-silica interface at room temperature, respectively. The difference in contact angles may lead to a slight curvature change at the colloidal particles near the wall during solvent evaporation. The particle-packing arrangement of the deposited assemblies was examined by a field-emission scanning electron microscope (JSM-6700F, JEOL, Japan). Only the deposition sections near the center of the patterned wafers were examined for comparison reasons.

Results and discussion

Effect of evaporation temperature on template-assisted convective assembly of latex spheres

Figure 2 shows typical SEM images of the colloid assemblies deposited at three different working temperatures (30, 45, and 65 °C, respectively) when the ratio of sphere diameter to groove width (D/W) was held at 0.12. The micrographs reveal that formation of ordered particle-packing structure in the confined grooves becomes more favorable at 45 °C with apparently fewer defect populations than those from other temperatures examined. At a reduced evaporation temperature of 30 °C, it appears that most polystyrene particles would rather stay on the substrate surface than fill into the rectangular channels (Fig. 2a). One is generally believed that a two-stage mechanism is involved in the convective self-assembly of colloidal spheres [4, 13]. Liquid at first forms a meniscus at the liquid–substrate interface. The liquid layer becomes "thinner" due to solvent evaporation, resulting in protrusion of the top of some spheres from the liquid layer. Menisci then form around the protruding tops of the colloidal spheres. Evaporation from these menisci further increases the local curvature, forming nucleus by the capillary attraction at the liquid–substrate interface [9]. The formation of nucleus is followed by a solvent influx from the thick portion of the liquid to the interface (thin region), rendering a convective flow in the liquid to alleviate stresses arising from the concentration gradient. This influx brings latex spheres to locations near the nucleuses, leading to the growth of arrayed colloids in close-pack lattice structure on flat surfaces. The use of patterned substrate yet induces an additional geometrical variable into the assembly process. The existence of groove walls physically changes the shape of menisci and breaks the balanced symmetry of capillary force at the liquid–substrate interface [9, 14, 15]. This unbalanced lateral (horizontal) force in turn carries the spheres into the grooves by fluid flow and may have also help in facilitating re-arrangement of particles within the grooves. The inability for the latex particles to enter into the grooved channel at 30 °C is then presumably due to a rather weak lateral force because of a low evaporation rate, and hence a reduced difference in the unbalanced capillary force. The magnitude of the capillary attraction stems from the surface tension of liquid used, the radius of contact line at the surface of the spheres, and the interparticle distance as well [4].

In contrast, when the temperature was raised to 65 °C, a vast amount of the latex particles preferred to enter into the grooves of the patterned substrate because of the drops of solvent are pinned in the groove [9] that induce strong horizontal driving forces on the particles to accumulate in the grooves. The relatively high evaporation temperature further induces a fast evaporation of solvent and a more intense solvent in-flux near the interface. Almost all the polystyrene particles fill into the grooves, and not on the top of the gratings. Visible packing defects accompany the formation of double-layered packing structure in the confined channels (Fig. 2c). It is possible that the increased evaporation temperature may have restricted the particles from re-arranging themselves into the most energetically favorable, 2D-hexagonal configuration. Additionally, Ye et al. [16] have shown that an intricate balance in the processes of nucleus formation, particle transport, and

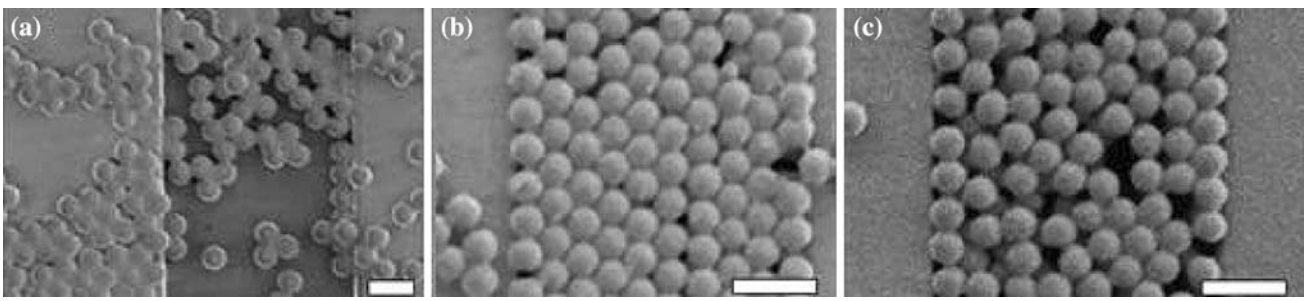

Fig. 2 SEM images of 482-nm latex spheres deposited on grooved substrates at different temperatures. (**a**) 30 °C, (**b**) 45 °C, and (**c**) 65 °C (0.01 vol.% solution, $W = 4000$ nm, $H = 550$ nm, scale bar is 1000 nm)

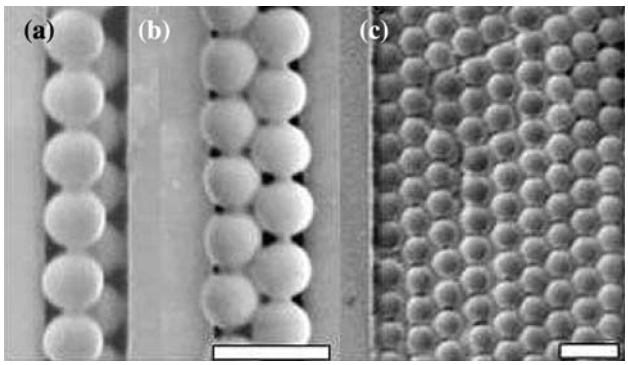

Fig. 3 SEM images of 482-nm latex spheres deposited on grooved substrates of various grating widths. $W = 650$ nm for both (**a**) and (**b**), $W = 4000$ nm for (**c**) (0.01 vol.% solution, $H = 550$ nm, evaporation temperature 45 °C, scale bar is 1000 nm)

crystallization is required to grow high-quality colloidal crystals via the vertical deposition method. A fast crystal growth rate due to the increase of evaporation temperature would spoil the balance and result in defects formation.

Effect of *D*/*W* ratio on template-assisted convective assembly of latex spheres

Figure 3 shows particle-packing configurations when the groove width was varied. The microsphere size ($D = 482$ nm) and the evaporation temperature (45 °C) were held constant. When $D/W = 0.74$, free space in the grooves allowable for the spheres to fill in was limited. Two sets of particle-packing arrangement resulted. Figure 3a shows one of them, in which a packing structure with two-layered single row of particle arrangement was found. The latex particles on the top layer sit exactly at the interstices of the underneath particles array and lean toward the other side of the groove wall, when compared to that of the bottom row of particles. Figure 3b shows the other set of particle-packing structures, in which an additional row of particles fills in the interstices available on the top layer of the particles arrays. The above particle-packing arrangements are apparently influenced by the confined wall during convective self-assembly. It has been stated in the previous section that the patterned grooves physically change the shape of menisci between the top of the protruding particles in the nucleus and break the balanced symmetry of capillary force at the liquid–substrate interface. This unbalanced lateral force brings the latex spheres into the grooves by fluid flow. The evaporation of water in the grooves induces a horizontal capillary force to re-arrange the particles within the grooves. Yet, the confined groove width with a *D*/*W* ratio of 0.74 restrains them from undergoing an effective re-arrangement, leading to the formation of a less dense structure in some areas when the particle transport is presumably slower than the

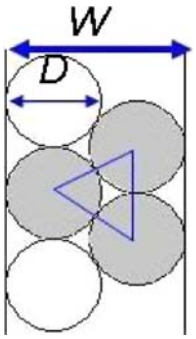

Fig. 4 A geometrical illustration showing *D*/*W* ratio for a 2D hexagonal, arrayed spheres

crystallization rate. In contrast, when the groove width is further increased to $D/W = 0.12$ (Fig. 3c), arrayed crystals with a 2D hexagonal structure form in the grooves, due mostly to a more relaxed wall effect so that an increased freedom for particle re-arrangement became operative.

A geometrical model is used to calculate the "critical" *D*/*W* ratio for attaining a 2D close-packing structure of spheres on flat surface with a given width. In Fig. 4, the gray spheres are the smallest "unit element" to assemble themselves into a hexagonal packing structure. For this coplanar structure, W scales with D in a form that $W = \frac{2+\sqrt{3}}{2}D$. This hence gives a "critical" *D*/*W* ratio of 0.54. For *D*/*W* ratios smaller than this value, i.e., $D/W < 0.54$, capillary interaction predominates the arraying of particles during solvent evaporation and induces particle re-arrangement within a given groove width W. The re-arrangement is particularly pronounced when the *D*/*W* ratio becomes much smaller than the critical value, leading to the formation of hexagonal packing structure. The geometrical model yet implicitly assumes that the asymmetric capillary forces imposed by the confined walls can be neglected, which is expected to be true only at small *D*/*W* ratios. In contrast, for $D/W > 0.54$, the particle re-arrangement is prohibited to an undetermined degree. This gives rise to a formation of a range of non-close-packing structures depending on process variables such as local sphere concentration near the liquid–substrate interface. The geometrical model is indeed not unique. In addition to the negligence of the confined wall effect, the model does not account for process variables such as evaporation temperature. As shown in Fig. 2 where the *D*/*W* ratio was held at 0.12 for all the temperatures examined, different structures were resulted. Nonetheless, the geometrical model still reasonably explains the various packing structures obtained in Fig. 3 when given *D*/*W* ratios were used.

Effect of *D*/*H* ratio on template-assisted convective assembly of latex spheres

Figure 5 shows different particle-packing arrangements when the sphere size was varied while the depth and width

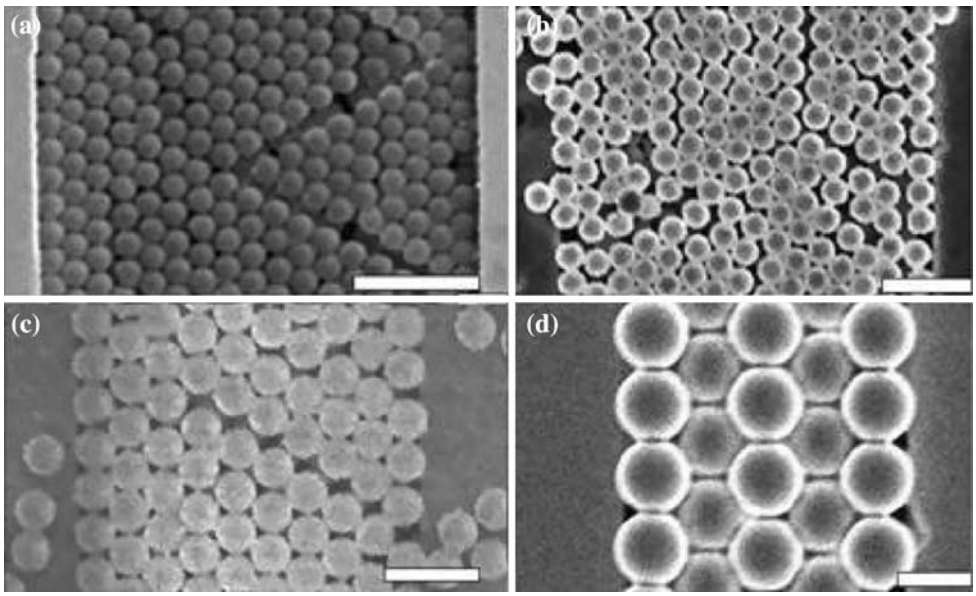

Fig. 5 SEM images of latex spheres deposited on grooved substrates when colloidal spheres of different diameters were used. (**a**) 262 nm, (**b**) 300 nm, (**c**) 482 nm, and (**d**) 1000 nm (0.01 vol.% solution, $H = 550$ nm, $W = 4000$ nm, evaporation temperature 45 °C, scale bar is 1000 nm)

of the rectangular grooves were both held constant, i.e., $H = 550$ nm and $W = 4000$ nm, respectively. The sphere sizes all satisfy the geometrical D/W ratio ≤ 0.54 requirement for the particle re-arrangement within the confined channels. The ratio of sphere size versus groove height (or depth), i.e., D/H, yet varied from 0.48 to 1.82. In Fig. 5a–c, latex spheres with D/H ratios of 0.48–0.88 favor to form a single-layered or double-layered, coplanar packing configuration within the grooves. When the sphere diameter is increased to be greater than the groove depth, i.e., $D/H = 1.82$, the assembled arrangement changed from the coplanar array to a non-coplanar, double-layered packing arrangement (Fig. 5d).

A model is proposed to explain the experimental findings. As shown in Fig. 6a, latex particles with a reduced D/H ratio smaller than unity possess a higher degree of freedom in re-arranging themselves to form a more energetically favorable particle arrangement with a dense packing configuration, resulting in the formation of single-layered or double-layered coplanar structure in the confined microgrooves with no apparent extra particles left behind on the dried substrate surface. This compares quite favorably with the observations in Fig. 5, especially when the D/H ratio is much smaller than unity. In contrast, as $D/H > 1$, two particle-packing arrangements may form. As shown in Fig. 6b and c, the number of particles able to be arranged within the grooves is limited as the physical size of the particles is increased. Additional row of particles on top of the arrayed packing spheres then possesses a total packing height exceeding that of the groove wall so that the particles are more easily to be pulled away by capillary forces to the positions from the groove to the free substrate surface during drying. The capillary force involved in Fig. 6b might have been smaller than that involved in Fig. 6c because the liquid-front line calculated from the total height of the double-layered packing configuration is slightly smoother than that of the other arrangement. A significant portion of the spheres near the edge of the groove wall exceeds the groove height in Fig. 6c and thus induces a pronounced capillary force on the particles with

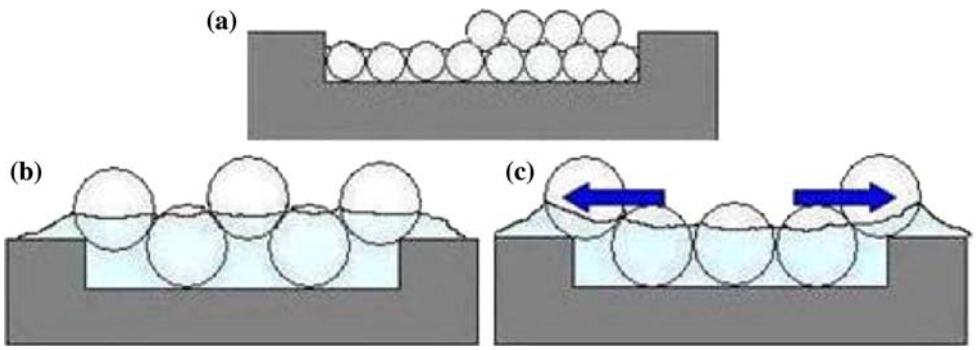

Fig. 6 Schematic cross-sectional drawings of the arrangement of latex spheres in the groove with various D/H ratios. (**a**) $1/3H < D < H$, (**b**) $D > H$ (stable), and (**c**) $D > H$ (unstable)

the increased curvature so the outer spheres on the top layer tend to depart from the groove or change their configuration to Fig. 6b if possible.

Conclusion

Self-assembly of mono-sized polystyrene particles was conducted on patterned silicon wafers with 1D grating, rectangular microgrooves via a convective evaporation method. Physical confinements together with capillary interactions involved at the liquid–substrate interface critically determine the assembled particle arrangement upon solvent evaporation, resulting in various particle-packing arrangements mainly determined by the capability of particle re-arrangement from the confined wall effect. An intricate balance in the processes of nucleus formation, particle transport, and crystallization is a key to grow ordered opals via the colloidal route. In this study, evaporation temperature of 45 °C appears to be a favorable deposition temperature. The geometrical restriction imposed on the latex particles by the confined walls becomes more significant when the D/W ratio exceeds a critical value of 0.54 or when the D/H ratio is greater than unity, leading to various packing configurations different from the hexagonal packing arrangement.

Acknowledgement Financial support from the National Science Council (Taiwan, ROC) under contract 92-2216-E-005-021 is gratefully acknowledged.

References

1. Park S, Qin D, Xia Y (1998) Adv Mater 10:1028. doi:10.1002/(SICI)1521-4095(199809)10:13<1028::AID-ADMA1028>3.0.CO;2P
2. Holgado M, Garcia-Santamaria F, Blanco A, Ibisate M, Cintas A, Miguez H et al (1999) Langmuir 15:4701. doi:10.1021/la990161k
3. Vlasov YA, Bo X-Z, Sturm JC, Norris DJ (2001) Nature 414:289. doi:10.1038/35104529
4. Denkov ND, Velev OD, Kralchevsky PA, Ivanov IB, Yoshimura H, Nagayama K (1992) Langmuir 8:3183. doi:10.1021/la00048a054
5. Yin Y, Lu Y, Gates B, Xia Y (2001) J Am Chem Soc 123:8718. doi:10.1021/ja011048v
6. Hoogenboom JP, Rétif C, de Bres E, van de Boer M, van Langen-Suurling AK, Romijn J et al (2004) Nano Lett 4:205. doi:10.1021/nl034867h
7. Ozin GA, Yang SM (2001) Adv Funct Mater 11:95. doi:10.1002/1616-3028(200104)11:2<95::AID-ADFM95>3.0.CO;2-O
8. Yang SM, Míguez H, Ozin GA (2002) Adv Funct Mater 12:425. doi:10.1002/1616-3028(20020618)12:6/7<425::AID-ADFM425>3.0.CO;2-U
9. Ye Y-H, Badilescu S, Truong V-V, Rochon P, Natansohn A (2001) Appl Phys Lett 79:872. doi:10.1063/1.1391234
10. Joannopoulos JD, Villeneuve PR, Fan S (1997) Nature 386:143. doi:10.1038/386143a0
11. Krauss TF, De La Rue RM (1999) Prog Quantum Electron 23:51. doi:10.1016/S0079-6727(99)00004-X
12. Aoki K, Miyazaki HT, Hirayama H, Inoshita K, Baba T, Sakoda K et al (2003) Nat Mater 2:117. doi:10.1038/nmat802
13. Dimitrov AS, Nagayama K (1996) Langmuir 12:1303. doi:10.1021/la9502251
14. Lin KH, Crocker JC, Prasad V, Schofield A, Weitz DA, Lubensky TC et al (2000) Phys Rev Lett 85:1770. doi:10.1103/PhysRevLett.85.1770
15. Aizenberg J, Braun PV, Wiltzius P (2000) Phys Rev Lett 84:2997. doi:10.1103/PhysRevLett.84.2997
16. Ye YH, LeBlanc F, Haché A, Truong V-V (2001) Appl Phys Lett 78:52. doi:10.1063/1.1337619